SYSTEM SAFETY: HUMAN - TECHNICAL FACILITY – ENVIRONMENT
7(1), 2025, pp. 578-597

EFFECT OF PIN-HOLE ON THE PERFORMANCE OF LOW TEMPERATURE PROTON EXCHANGE MEMBRANE FUEL CELL FOR DIFFERENT FLOW FIELDS AND CATALYST LOADINGS

DOI: 10.2478/czoto-2025-0053
Received: 04/11/2025
Accepted: 13/12/2025

Sudesh Bekal[1,2] – *orcid id:000-0002-8058-5410, e-mail: sudeshbekal@nitte.edu.in*
[1]NMAM Institute of Technology, Nitte-574110, Karnataka, **India**
[2]NITTE deemed to be university, Deralakatte, Mangaluru, Karnataka, **India**

Abstract: This study investigates the impact of membrane pinholes on the performance of PEMFCs by analyzing the results obtained using novel flow field designs, in comparison with first generation flow fields. The tests were carried out at the optimal hydrogen-to-oxygen ratio that yielded maximum power output, across three different hydrogen flow rates. The experiments indicated that a pinhole in the membrane reduces fuel cell performance across all 10 configurations studied (combinations of flow field types and catalyst loadings). Specifically, the twin-inlet twin-outlet flow field, the conventional serpentine flow field, and the 2 mm circular cavity flow field failed to deliver meaningful output in most cases when a pinhole was present. In contrast, the 6 mm (CCFF-6 mm) and 4 mm (CCFF-4 mm) circular cavity flow fields maintained substantial power output under the same conditions, with CCFF-6mm demonstrating superior performance. The Tafel slope analysis indicated that the CCFF-6 mm configuration outperformed all other designs in terms of electrochemical behavior.
Keywords: pin-hole defect, durability, maximum power point, voltage over potential

1. INTRODUCTION

Fossil fuels are finite in nature and, during their continued use in the interim, contribute significantly to global warming and localized environmental pollution. To mitigate these issues, renewable energy sources such as solar, wind, and tidal power are increasingly being explored. However, these technologies are capital-intensive, necessitating the identification of alternative energy solutions.

Hydrogen emerges as a promising clean fuel with substantial potential to reduce pollution and support sustainable development. It can be efficiently utilized in proton exchange membrane fuel cells (PEMFCs) to generate electricity directly from chemical energy with relatively high efficiency. Fuel cells are used for many applications such as mobile and stationary power generation and including stationary power generation and for power supply for electronic devices.

During operation, the membrane of a proton exchange membrane fuel cell (PEMFC) is subjected to multiple forms of degradation, including chemical and mechanical deterioration. To maintain efficiency and ensure long-term durability, the membrane must preserve both its electrochemical and mechanical integrity. However, operational stresses – arising from chemical reactions and mechanical strain – can accelerate the creation of pinholes in the membrane (Moukheibe et al. 2014)

Pinholes are small, through-the-thickness defects in the PEM that significantly impair the fuel cell's performance and longevity. These defects often result from hydrothermal stresses induced by fluctuations in temperature and humidity during operation (Tang et al., 2006; Kusoglu et al., 2006; Meredith et al., 2011; Lai et al., 2009; Silberstein & Boyce 2011). (De et al. 2012) reported the occurrence of linear cracks aligned with the direction of gas flow, further compromising membrane integrity. Additionally, the dissolution and recrystallization of platinum catalysts contribute to membrane embrittlement (Zhang et al., 2009).

Among various degradation mechanisms, mechanical failure – manifesting as perforations, cracks, tears, or pinholes – is one of the leading causes of premature membrane failure (Collier et al., 2006). Dimensional changes resulting from inadequate humidification, low humidity conditions, and relative humidity cycling have also been shown to adversely affect mechanical durability (Büchi and Srinivasan, 1997; Yu et al., 2005; Endoh et al., 2004;Yu. 2005).

These mechanical instabilities facilitate gas crossover, which not only causes undesirable heat and water generation but also leads to energy loss (Nguyen and Fushinobu, 2020). Furthermore, gas crossover accelerates the degradation of both the membrane and electrodes, particularly under hydrogen starvation conditions. This can result in a reduction of active platinum catalyst surface area and degradation of the carbon support structure (Bodner et al., 2015; Chippar et al., 2014). Localized heat generation may also create hotspots, posing potential safety risks.

Pinhole defects can accelerate the chemical decomposition of the polymer membrane, ultimately leading to fuel cell failure. Therefore, early detection and accurate characterization of pinhole degradation are essential. Previous studies (Ding et al., 2023) have identified the formation of localized reverse currents and hotspots in the vicinity of pinholes, highlighting their detrimental effects. (Chen et al.,2025) used a numerical model to study the effect of pin hole size on hydraulic leakage within PEMFC and inlet pressure on the performance. According to them, if inlet pressure is maintained constant, pin hole smaller than 0.37 mm diameter exhibit minimum impact on the fuel cell performance.

Physics-based modeling approaches are used to understand membrane deterioration and the interdependent relationship between durability and performance (Ehlinger et al., 2019). Simulation results reveal that pinholes tend to grow under relative humidity cycling, which leads to increased gas crossover and a corresponding decline in fuel cell performance.

Moreover, the modeling underscores the nonlinear behavior of membrane degradation and emphasizes the necessity of integrating both mechanical and chemical degradation mechanisms. Such coupled models are crucial for accurately capturing the membrane's degradation behavior under various operational conditions, and they provide a foundational framework for evaluating the trade-offs between durability and performance.

It is of particular interest to investigate whether the use of specialized flow field designs can yield improved performance compared to the conventional serpentine flow field, especially under conditions where pinhole defects are present in the membrane. It is believed that an appropriate flow field will have little influence in causing further

deterioration of the membrane which is already possessed of pin-hole. An additional objective of this study is to compare efficiency of the fuel cell across ten different flow field configurations, with the aim of identifying the most effective design.
To achieve this, key performance metrics – including power output, peak power, limiting current density, maximum power point, open-circuit voltage (OCV), and polarization behavior – are systematically compared across all configurations.
In this study, artificial pinholes were introduced into the membrane, and experiments were conducted using various specialized flow field designs to evaluate whether reasonable performance could be sustained over the duration of testing. The performance of these configurations was then compared to that of a PEMFC employing the conventional serpentine flow field. This comprehensive investigation considers multiple factors, including hydrogen flow rates, different catalyst loading ,different variants of circular cavity flow fields, the twin-inlet twin-outlet flow field, and the conventional serpentine flow field.

2. EXPERIMENTAL METHODOLOGY

The experiments focus on evaluating the performance of a PEMFC with a pinhole defect using three different flow field configurations: (i) circular cavity-type flow field, (ii) twin-inlet twin-outlet flow field, and (iii) conventional serpentine flow field. Performance comparisons are based on polarization behavior, peak power output, limiting current density, and voltage overpotential.
The scope of the study is limited to short-duration operation, with experiments conducted up to the point of limiting current density when pinholes are developed in the MEA. Within this framework, the observed performance serves as an indicator of the membrane's durability. A more rigorous and long-term assessment of durability remains a subject for future research.
The following section outlines the experimental methodology in detail.

2.1 Scheme of experiments

The primary objective of the experiments was to determine the performance of a PEMFC when pinhole defects are present in its membrane. The overall scheme of experimentation is shown in Fig.1. To design the experimental conditions, data from previous studies, where PEMFC performance was evaluated under various conditions were utilized. These conditions included different catalyst loadings (0.20 mg/cm², 0.25 mg/cm², 0.40 mg/cm², and 0.50 mg/cm²), varying levels of excess oxygen supply (0%, 50%, 100%, and 150%), different hydrogen flow rates (80 ml/min, 100 ml/min, and 120 ml/min), and multiple flow field configurations (CCFF-2 mm, CCFF-4 mm, CCFF-6 mm, twin-inlet twin-outlet flow field (TITOFF), and the conventional serpentine flow field (CSFF).
From this dataset, the optimal excess oxidant level corresponding to the maximum power output for each hydrogen flow rate was identified. Experiments involving pinhole defects were then conducted at these optimal conditions. For instance, in the case of a hydrogen flow rate of 80 ml/min and higher catalyst loading, the previous data showed maximum power outputs of 760 mW, 774 mW, 675 mW, and 714 mW for 0%, 50%, 100%, and 150% excess oxygen, respectively, using the CCFF-6 mm configuration. Accordingly, subsequent pinhole experiments were conducted at 50% excess oxidant supply for this case. During the experiments, voltage and power outputs were measured under various load conditions. From the resulting polarization and power curves, key performance

parameters such as open-circuit voltage (OCV), voltage over-potential, maximum power, limiting current density, and the maximum power point were extracted and analyzed.

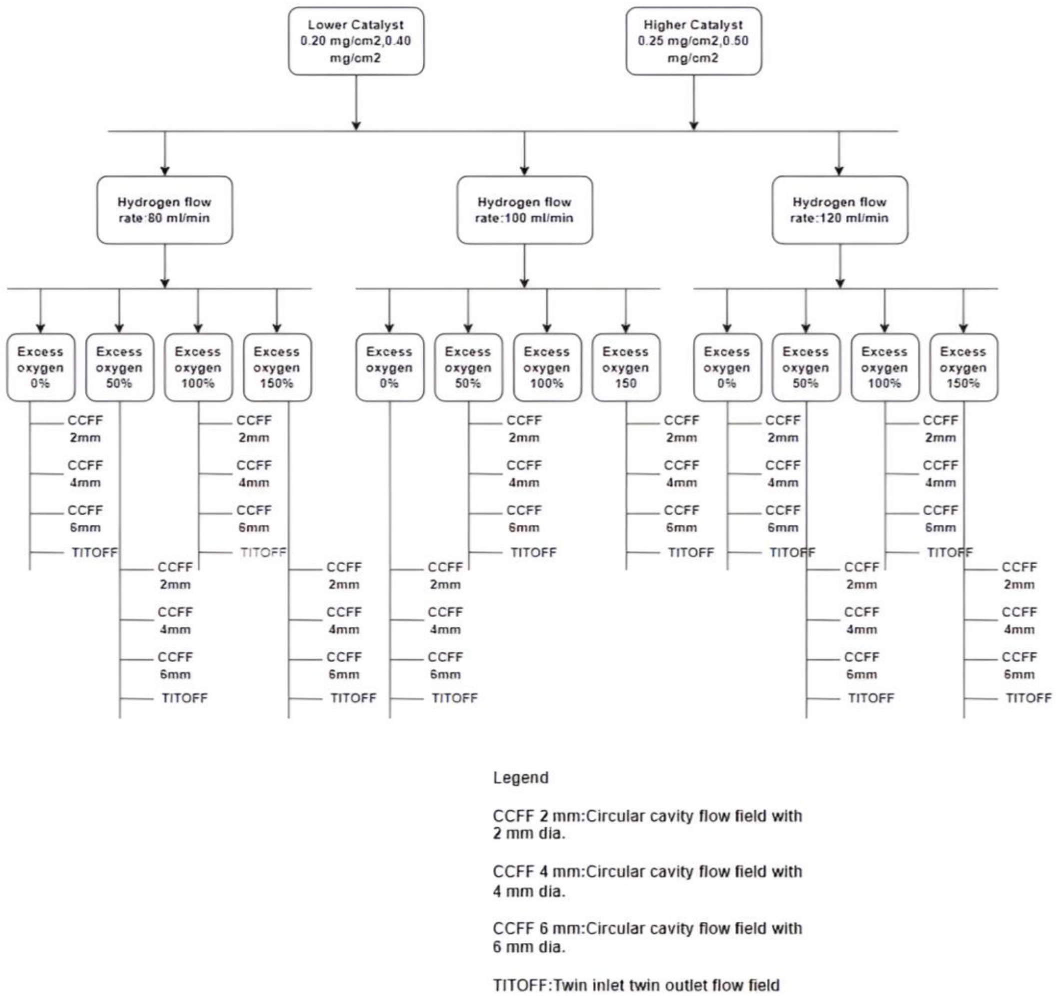

Fig. 1. Scheme of experimentation.

2.2 Experimental setup

Fuel Cell Workstation:

The experimental setup consists of a fuel cell test station, a fuel cell unit, an electronic load, a computer workstation, and gas pipelines equipped with flow regulators and pressure gauges. A schematic representation of the setup is shown in Fig. 2.

Fuel Cells:

This research investigates the performance behavior of proton exchange membrane fuel cells (PEMFCs) utilizing specialized flow field designs in the presence of pinhole defects in the membrane electrode assembly (MEA). To facilitate this study, two types of custom fuel cells were fabricated, each incorporating bipolar plates with unique flow field geometries:

(i) Circular Cavity Flow Field (CCFF) and

(ii) Twin-Inlet Twin-Outlet Flow Field (TITOFF).

The setup comprises the following components:

Humidifiers:

The fuel cell test station is equipped with two separate humidifiers, one for hydrogen and the other for oxygen. Gases are supplied from a centralized gas bank through a butterfly valve, pressure gauges, and flow regulators. A mass flow controller integrated within the test station ensures accurate gas flow rates, as defined by the user via the control software, and directs the gases to their respective humidifiers. Each humidifier is fitted with an electric heater, the temperature of which is precisely regulated through the software interface.

The software dashboard allows for real-time monitoring and adjustment of humidification temperatures for both hydrogen (H_2) and oxygen (O_2), along with the line temperatures of the gas supply streams.

Computer Workstation:

The computer interfaces with the master control unit of the fuel cell test station, which is governed by Proportional-Integral-Derivative (PID) controllers. These controllers dynamically regulate the heating elements by comparing the actual temperature to the set point and continuously adjusting output to minimize deviations, thereby ensuring thermal stability throughout the operation.

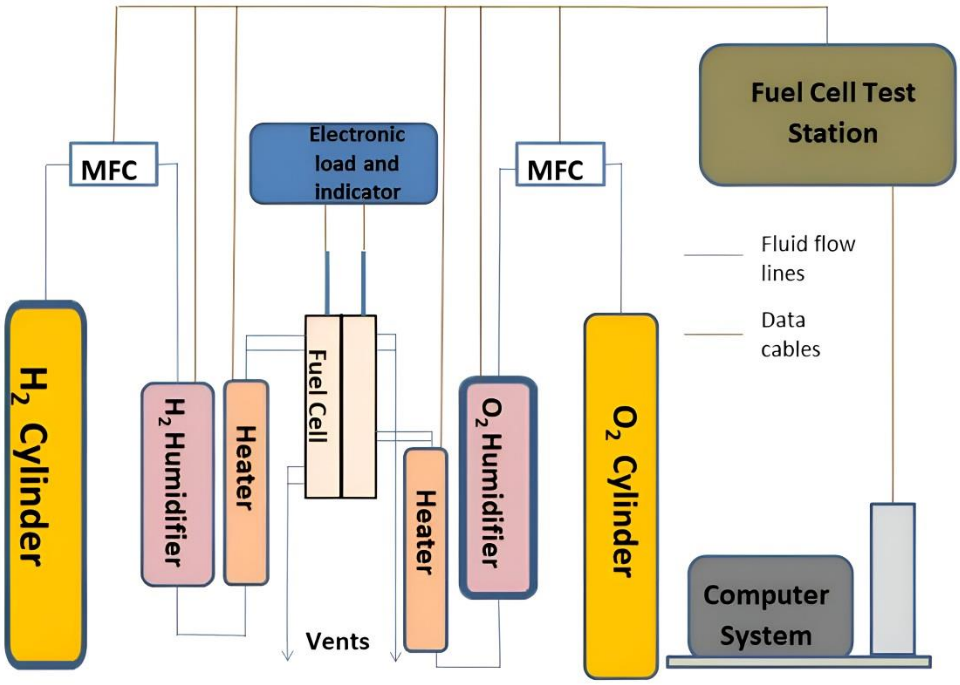

Fig. 2. Schematic diagram of the experimental setup used for PEMFC testing. The setup includes a fuel cell test station with integrated humidifiers for hydrogen and oxygen, a computer-controlled mass flow controller, pressure gauges, flow regulators, and an electronic load. A computer workstation interfaces with the system for real-time control and monitoring of temperature, flow rate, and cell performance parameters.

A schematic of the circular cavity flow field is presented in Fig. 3. This design consists of multiple circular cavities machined into a metallic plate, which is integrated into a bipolar plate. The bipolar plate includes provisions for gas inlet and outlet, enabling the reactant gases to enter, flow through, and exit via the engraved circular cavities.

Three variations of the circular cavity flow field were developed using different cavity diameters such as 2 mm, 4 mm, and 6 mm as illustrated in Fig. 4. Each of these flow field plates has a uniform thickness of 2 mm.

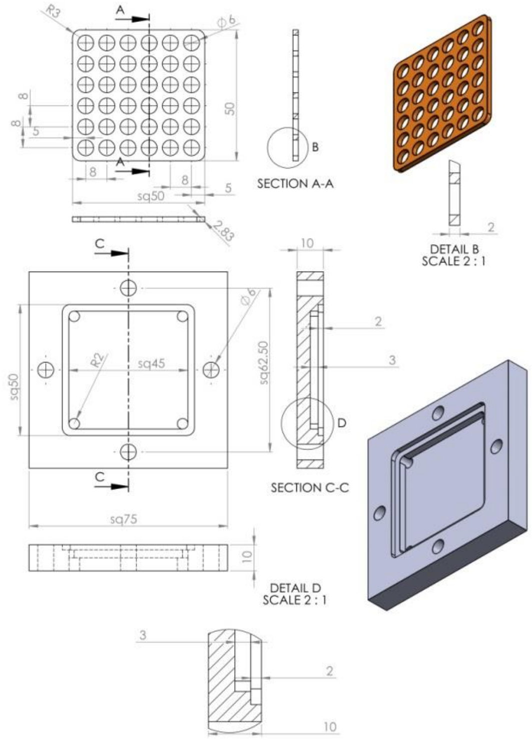

Fig. 3. Drawings of the circular cavity flow field (CCFF) design used in the bipolar plate. The design features multiple circular cavities through which the reactant gases flow, enabling uniform distribution across the membrane surface. (The drawing is for 6 mm diameter flow field. All dimensions are in mm)

These plates sit flush in the slot provided in the bipolar plate. The bipolar plate has outer dimension of 10 mm * 75 mm and houses a chamber of dimension 45 mm * 5 mm chamber with a step of 2 mm width and 2 mm height above it to hold the plate having circular cavities.

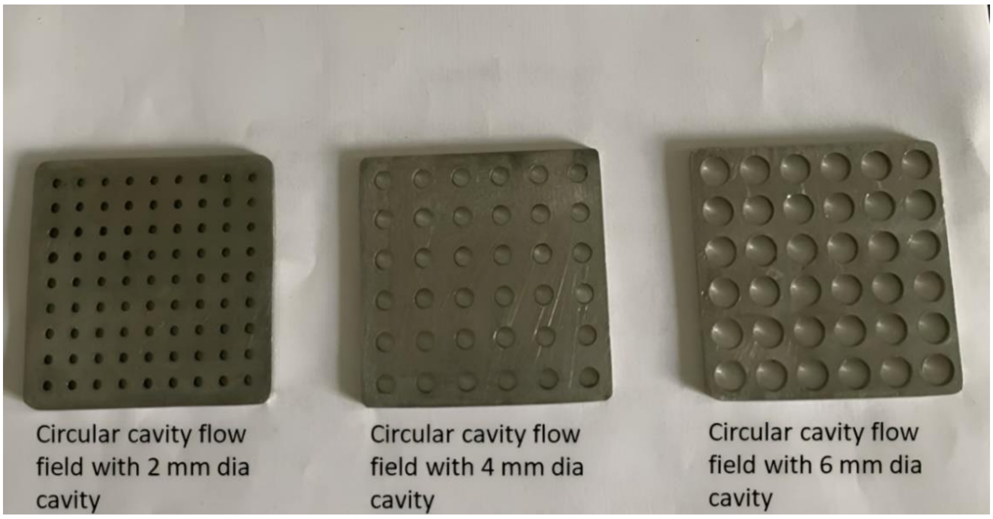

Fig. 4. Variants of circular cavity flow field plates with cavity diameters of 2 mm, 4 mm, and 6 mm. Each plate is 2 mm thick and designed to study the effect of cavity size on fuel cell performance in the presence of pinhole defects. Circular cavity plates to be used with bipolar plates(circular cavity with 2 mm,4 mm and 6 mm)

The second specialized flow field configuration is illustrated in Fig. 5. This bipolar plate is fabricated from stainless steel (SS) and features a twin-inlet twin-outlet flow field design, which enables the use of two separate gas channels. The overall dimensions of the bipolar plate are 10 cm × 10 cm, with the flow field occupying a central area of 5 cm × 5 cm matching the active area of the membrane electrode assembly (MEA).

The flow field comprises two independent channels of different lengths: one channel measures 567 mm and the other 467 mm. This configuration is designed to enhance gas distribution and potentially improve fuel cell performance under varying operational conditions.

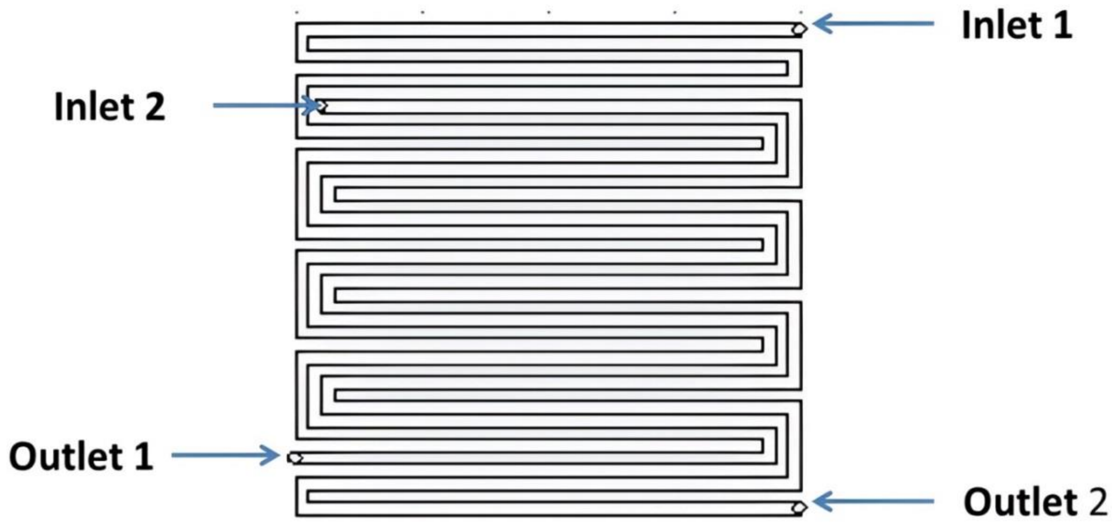

Fig. 5 Schematic of the twin-inlet twin-outlet flow field (TITOFF) bipolar plate made of stainless steel. The flow field occupies a 5 cm × 5 cm area at the center of a 10 cm × 10 cm plate and contains two independent channels measuring 567 mm and 467 mm in length, respectively, to facilitate improved reactant gas distribution across the MEA.

The two channels in the twin-inlet twin-outlet flow field are designed such that each channel has a dedicated inlet and outlet. The gas enters through its respective inlet, travels along the designated channel, and exits through a separate outlet. This configuration effectively divides the overall flow path into two distinct, parallel channels. By shortening the individual path lengths, the pressure drop across each channel is reduced compared to a single-channel design of equivalent total length. This reduction in pressure loss facilitates improved gas transport and enhances uniform gas distribution across the membrane surface. Additionally, the inlets of the two channels are laterally offset by 150 mm, further contributing to balanced flow distribution across the active area of the membrane electrode assembly (MEA).

In the first channel, gas flow over an initial length of 100 mm results in a measurable pressure drop. At this point, the gas also begins to enter the inlet of the second channel. Due to rim convection, a portion of the flow from the second channel recirculates into the first channel, partially restoring its pressure. As a result, the gas pressures in both channels tend to equalize at this junction. Beyond this point, the two channels run parallel to each other, promoting a uniform pressure distribution across the membrane electrode assembly (MEA).

As illustrated in Fig. 5, the gas in the first channel exits the flow field 100 mm before the gas in the second channel. This additional distance traversed by the gas in the second channel leads to a further continuous pressure drop. This gradual decline in pressure assists in displacing moisture accumulated within the channel. Consequently, this flow field design not only ensures uniform pressure across most of the MEA but also enhances water management by facilitating the removal of excess moisture.

Overall, this configuration is expected to improve fuel cell performance, particularly under conditions of reduced catalyst loading, by minimizing pressure losses and optimizing gas distribution within the cell.

Electronic load: The electronic load utilized in the setup can handle a maximum current of 40 A and power levels of up to 400 W, allowing for precise loading of the fuel cell during experiments. The electronic loading unit features a display that indicates voltage output, applied current, and power output.

Pin-hole Fabrication:

The membrane electrode assembly (MEA) used in this study was deliberately modified to simulate adverse operating conditions by introducing artificial pinhole defects. Pinholes with a diameter of 100 micrometers were introduced at the hydrogen inlet region of the MEA. In the case of the Twin-Inlet Twin-Outlet Flow Field (TITOFF) configuration, where two separate hydrogen inlets are present, two distinct
areas on the MEA were pierced with pinholes, as illustrated in Fig. 6. Conversely, for the Circular Cavity Flow Field (CCFF) configuration, which features only a single

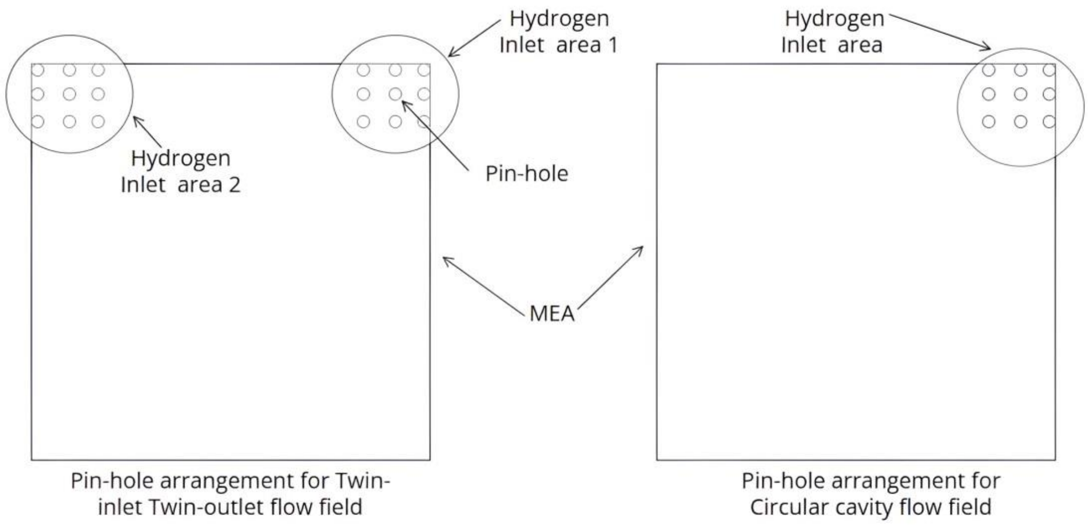

Fig. 6 Locations of 100 μm pinholes introduced in the membrane electrode assembly (MEA) for different flow field configurations. Two pinhole regions are shown for the Twin-Inlet Twin-Outlet Flow Field (TITOFF), corresponding to its two hydrogen inlets, while a single pinhole region is shown for the Circular Cavity Flow Field (CCFF), which has only one hydrogen inlet.

Hydrogen inlet, pinholes were introduced in only one corresponding region of the MEA.
A microstructural view of the modified MEA at 40X magnification is shown in Fig. 7, clearly displaying the 100-micrometre pinholes introduced for the study.

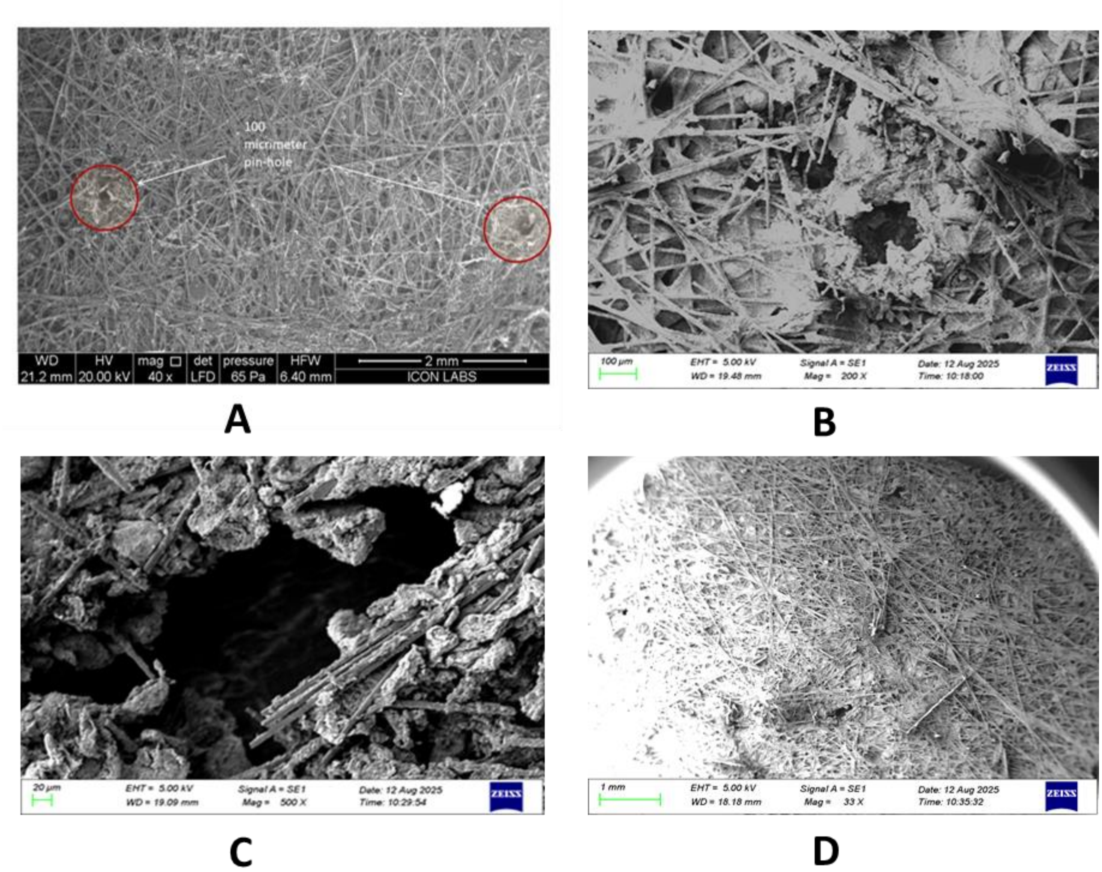

Fig. 7 Microstructural image of the membrane electrode assembly (MEA) at 40× magnification, showing artificially introduced pinholes of 100 μm diameter. These pinholes simulate mechanical degradation and allow evaluation of PEMFC performance under adverse operating conditions.

3. RESULTS AND DISCUSSION

The presence of a pinhole in the membrane creates a low-resistance pathway for hydrogen to crossover across MEA, disrupting normal electrochemical processes within the fuel cell. The hydrogen that crosses over bypasses the intended electrochemical reaction and directly reacts with oxygen at the cathode, producing water and heat. Consequently, this portion of hydrogen is no longer available for the standard electrochemical reaction, thereby reducing the overall efficiency and generation of power. Despite this inefficiency, a partial voltage is still generated due to the remaining hydrogen flowing through the anode channel. However, the heat generated by the unintended reaction at the cathode can lead to localized hotspots, which accelerate membrane degradation and reduce the durability of the fuel cell. The rate and extent of this deterioration depend on the magnitude of hydrogen crossover, which in turn is influenced by the flow field design and operating conditions. One of the main drawbacks which hinders the practical application of PEMFC is the durability which directly effects the cost of operation. If some improvement could be made by the use of special type of flow field, in the performance even after pin-hole is produced in the MEA, the fuel cell can be used for longer period, thereby reducing the cost of operation.

The present study aims to evaluate the impact of pinhole defects on PEMFC performance and durability when using different specialized flow field configurations. The flow field types investigated include:

(i) Circular Cavity Flow Field with 6 mm diameter cavities (CCFF-6 mm),
(ii) Circular Cavity Flow Field with 4 mm diameter cavities (CCFF-4 mm),
(iii) Circular Cavity Flow Field with 2 mm diameter cavities (CCFF-2 mm),
(iv) Twin-Inlet Twin-Outlet Flow Field (TITOFF), and
(v) Conventional Serpentine Flow Field (CSFF).
Two types of membrane electrode assemblies (MEAs) were tested:
(i) MEAs with lower catalyst loading and
(ii) MEAs with higher catalyst loading.
The fuel cells were operated under varying hydrogen flow rates of 80, 100, and 120 ml/min, with oxygen flow rate in proportion of 50%, 75%, 100% and 125% that of hydrogen flow rate resulting in excess oxygen proportion of 0, 50%, 100%, and 150%. During the course of experimentation, key performance parameters including open-circuit voltage (OCV), voltage overpotential, limiting current density, maximum power output, and maximum power point, were systematically recorded.
These performance metrics are presented in Table 1 and Table 2, corresponding to higher and lower catalyst loading conditions, respectively, across the various flow field configurations and hydrogen flow rates. As noted in Section 2.1, the reported values represent performance under the specific excess oxygen supply conditions that yielded the highest maximum power output for each hydrogen flow rate.

Table 1
The observations for different parameters for higher catalyst loading while operating MEA with pin-hole (NWD: not well defined; HCL: higher catalyst loading; CCFF: circular cavity flow field; OCV: Open circuit voltage; TITOFF: twin inlet twin outlet flow field; CSFF: conventional serpentine flow field)

Catalyst loading	**Flow field variant**	**H2 Flow rate (mL/min)**	**Excess O_2 (%)**	**OCV (volt)**	**Voltage over potential(volt)**			**Limiting current density (mA/cm^2)**	**Max. Power (mW)**	**Max. power point (mA/cm^2)**
					Activation	**Ohmic**	**Concent-ration**			
HCL	**CCFF-6**	80	50	890	417	297	0	120	774	80
		100	100	921	347	377	0	128	847	88
		120	50	890	236	445	0	120	818	80
	CCFF-4	80	150	976	317	500	0	112	743	72
		100	150	976	181	495	0	104	843	80
		120	150	940	299	384	0	104	770	80
	CCFF-2	80	150	922	342	457	0	48	274	24
		100	150	933	437	367	0	88	521	48
		120	150	987	481	381	0	56	324	32
	TITOFF	80	50	855	NWD	NWD	NWD	24	132	16
		100	150	807	NWD	NWD	NWD	24	146	16
		120	100	Not steady						
	CSFF	80	100	Not steady						
		100	150	Not steady						
		120	100	Not steady						

Table 2
The observations for different parameters for lower catalyst loading while operating with MEA with pin-hole (NWD: Not well defined; HCL: higher catalyst loading; CCFF: circular cavity flow field; OCV: Open circuit voltage; TITOFF: twin inlet twin outlet flow field; CSFF: conventional serpentine flow field)

Catalyst loading	Flow field variant	H2 Flow rate (mL/min)	Excess O_2(%)	OCV (volt)	Voltage over potential(volt)			Limiting current density (mA/cm²)	Max. Power (mW)	Maximum power point (mA/cm²)
					Activation	Ohmic	Concent-ration			
LCL	CCFF-6	80	100	970	299	562	0	128	737	64
		100	50	940	190	620	0	112	687	64
		120	150	916	316	423	0	120	771	72
	CCFF-4	80	50	1002	311	543	0	112	670	80
		100	0	983	409	378	0	120	809	80
		120	100	1013	299	530	0	120	795	80
	CCFF-2	80	150	980	320	529	0	96	590	56
		100	150	965	416	415	0	80	512	48
		120	150	952	379	465	0	96	560	48
	TITOFF	80	100	786	NWD	NWD	NWD	16	112	8
		100	150	647	NWD	NWD	NWD	16	81	8
		120	100	771	339	299	0	32	172	16
	CSFF	80	100	Not steady						
		100	100	Not steady						
		120	100					Not steady		

3.1 Flooding and fuel cell temperature when operating with MEA with pin-hole

An analysis of the data presented in Table 1 and Table 2 reveals that fuel cell operation with Circular Cavity Flow Fields (CCFFs) consistently yielded reasonably high values of open-circuit voltage (OCV) and maximum power output, even in the presence of pinhole defects. In contrast, fuel cells employing the Twin-Inlet Twin-Outet Flow Field (TITOFF) and the Conventional Serpentine Flow Field (CSFF) exhibited unstable or significantly reduced performance, with results often too erratic to be recorded reliably.

In the case of the TITOFF configuration with Lower Catalyst Loading (LCL) and a hydrogen flow rate of 80 ml/min, a substantial temperature rise was observed by the end of the experiment, reaching 45°C, compared to an ambient temperature of 30°C. Additionally, heavy flooding was noted in the cell. These phenomena suggest that significant hydrogen crossover may have occurred through the membrane pinholes, leading to a direct chemical reaction between hydrogen and oxygen at the cathode side. This reaction would produce excess water and heat, accounting for both the temperature increase and flooding.

Moreover, evidence of back diffusion of water into the anode side further supports the occurrence of excessive water generation. Similar issues were observed at 100 ml/min and 120 ml/min hydrogen flow rates, with fuel cell temperatures rising to 38.3°C and 36.3°C, respectively, under ambient conditions of 32.7°C and 33.5°C. The extent of flooding remained high under these conditions.

As a result of these adverse effects, the fuel cell voltage output under TITOFF and CSFF configurations showed random fluctuations, deviating from the typical polarization behavior. Consequently, voltage overpotential values could not be reliably determined in several test cases.

In the case of the Conventional Serpentine Flow Field (CSFF), the fuel cell exhibited unstable open-circuit voltage (OCV) across all tested hydrogen flow rates. The cell failed to sustain any external load due to severe operational instability. Heavy flooding was observed on both the cathode and anode sides, accompanied by a significant temperature rise reaching 42.8°C, compared to an ambient temperature of 35.4°C.

Similar behavior was also noted under higher catalyst loading, indicating that the serpentine design lacks the robustness needed to maintain performance in the presence of membrane pinhole defects.

As for CCFF, for CCFF-6 mm and higher catalyst loading, heavy flooding is found for 80,100 and 120 ml/min hydrogen flow rate in the cathode side; however, anode side collected little flooding. The flooding was less for 80 ml/min hydrogen flow rate, as the gas crossover is less due lesser flow rate of hydrogen. The fuel cell temperature for 80 ml/min was found to be 36.6°C(for 33.6°C ambient temperature), for 120 ml/min, it was 36.3°C (with ambient temperature of 30°C) and for 100 ml/min, it was 35.2°C (30°C). For 100 and 120 ml/min flow rates, the temperature evolved is more compared to 80 ml/min flow rate which indicates that hydrogen cross over is more for 100 and 120 ml/min, possibly due to higher flow rate.

For the Circular Cavity Flow Field with 6 mm diameter (CCFF-6 mm) under lower catalyst loading, only minimal flooding was observed. This can be attributed to the reduced number of active reaction sites at the cathode, resulting in less hydrogen-oxygen direct reaction due to crossover. This observation is further supported by the relatively low cell temperatures recorded at the end of each experiment:80 ml/min: 36.9°C (ambient: 33.9°C);100 ml/min: 36.8°C (ambient: 33.1°C);120 ml/min: 36.9°C (ambient: 33.9°C).

These modest temperature rises indicate limited parasitic reactions and effective water management in the presence of membrane pinholes.

In contrast, for the CCFF-4 mm configuration with higher catalyst loading, the results deviated from those of CCFF-6 mm. While light flooding was observed at 80 ml/min, heavy flooding occurred at 100 ml/min, and very heavy flooding was evident at 120 ml/min. The corresponding cell temperatures reflect this trend:

80 ml/min: 37.8°C (ambient: 32.8°C);100 ml/min: 42.5°C (ambient: 31.5°C);120 ml/min: 43.7°C (ambient: 33.9°C)

These elevated temperatures and flooding levels suggest that higher catalyst loading increases the number of active sites available for undesirable hydrogen-oxygen reactions at the cathode, particularly in the presence of pinholes. The resulting direct combustion produces substantial amounts of heat and water, exacerbating flooding and contributing to rapid performance degradation.

Overall, these findings highlight the importance of optimizing both flow field design and catalyst loading to balance reactivity, water management, and durability under compromised membrane conditions.

For the lower catalyst loading configuration, minor flooding was observed at hydrogen flow rates of 80 ml/min and 100 ml/min, with corresponding cell temperatures of:80 ml/min: 40.8°C (ambient: 34.8°C);100 ml/min: 41.3°C (ambient: 36.3°C);

These moderate temperature rises suggest a manageable level of hydrogen crossover and localized reaction. However, at 120 ml/min, heavy flooding was evident, accompanied by a significant temperature increase to 47.8°C (ambient: 36.1°C). This sharp rise is indicative of intensified hydrogen crossover and large-scale parasitic combustion at the cathode, leading to excessive water and heat generation.

For the CCFF-2 mm flow field with higher catalyst loading, very low flooding was noted across all tested flow rates. Cell temperatures remained close to ambient, reflecting stable operation:80 ml/min: 37.1°C (ambient: 34.2°C);100 ml/min: 36.3°C (ambient: 34.1°C);120 ml/min: 37.3°C (ambient: 33.2°C)

Despite this thermal stability, at 120 ml/min, a relative increase in flooding was observed on both the anode and cathode sides. Additionally, significant fluctuations in voltage and power output were recorded during the experiment. These irregularities may be attributed to local variations in membrane hydration, inconsistent gas distribution, or intermittent hydrogen crossover dynamics at high flow rates.

Overall, the data suggest that CCFF-2 mm with higher catalyst loading provides good water and thermal management, but electrical stability may be compromised under high flow rate conditions, warranting further investigation into flow uniformity and membrane resilience.

For the CCFF-2 mm flow field with lower catalyst loading, heavy flooding was consistently observed across all hydrogen flow rates. The recorded cell temperatures showed substantial deviation from ambient conditions, further indicating abnormal internal activity and poor water management:

80 ml/min: 41.1°C (ambient: 34.9°C)

100 ml/min: 44.1°C (ambient: 36.2°C)

120 ml/min: 42.7°C (ambient: 35.8°C)

At all tested flow rates, the fuel cell was unable to sustain external loads beyond very low values, rendering it practically non-operational. This performance degradation can be attributed to a combination of factors:

Restricted gas transport: The small diameter of the circular cavities limited the flow of reactants into the MEA, resulting in poor gas distribution.

Membrane defects: The presence of pinholes facilitated direct crossover of hydrogen to the cathode side, leading to parasitic chemical reactions and increased water generation.

Insufficient electrochemical activity: The lower catalyst loading further reduced the number of active reaction sites, compounding the inefficiency.

These combined effects led to excessive flooding, localized heat accumulation, and ultimately failure of the fuel cell to operate under load conditions. This configuration highlights the sensitivity of low-loading MEAs to both flow field geometry and defect-induced stress, reinforcing the importance of optimizing both design and material parameters.

To evaluate and compare the reaction kinetics of various flow field configurations, Tafel analysis was employed, as no advanced electrochemical impedance or diagnostic apparatus was available. Tafel plots were generated for three circular cavity flow field configurations such as CCFF-6 mm, CCFF-4 mm, and CCFF-2 mm, under both higher and lower catalyst loading conditions. Due to insufficient data from the TITOFF and CSFF configurations, Tafel slope values could not be determined for those cases.

The parameters derived from the Tafel plots are summarized in Table 3. Across all configurations, the observed Tafel slopes were relatively high, indicative of poor reaction kinetics. This can be attributed to two primary factors:
(1) the low operating temperatures, which inherently slow the electrochemical reaction rates, and
(2) the presence of pinholes in the membrane, which result in hydrogen crossover, leading to undesired side reactions and inefficient utilization of reactants.
A comparison between higher and lower catalyst loading reveals that, in most cases, higher catalyst loading correlates with lower Tafel slopes, suggesting improved chemical kinetics due to increased availability of active reaction sites. Conversely, for CCFF-4 mm and CCFF-2 mm, the use of lower catalyst loading significantly worsens the Tafel slope, reflecting poor catalytic activity, reduced efficiency, and the need for a higher over potential to achieve the same current density.
These findings reinforce the importance of both catalyst optimization and flow field design in sustaining efficient reaction kinetics, particularly under non-ideal operating conditions involving membrane degradation.

Table 3
Tafel Slope for Circular cavity flow field for MEA with pin-hole present (For other flow field such as TITO and CSFF not enough data were available for plotting the Tafel slope or data produced inappropriate values of Tafel slope)

	Flow field configuration								
	CCFF-6 mm			**CCFF-4 mm**			**CCFF-2 mm**		
Flow-loading Group	**Tafel Slope (mV/dec)**	**Intercept (mV)**	**R^2 (Goodness of Fit)**	**Tafel Slope (mV/dec)**	**Intercept (mV)**	**R^2 (Goodness of Fit)**	**Tafel Slope (mV/dec)**	**Intercept (mV)**	**R^2 (Goodness of Fit)**
80HCL	−545.65	124.26	0.901	−464.84	18.02	0.911	-505.05	32.11	0.91
100HCL	−526.55	114.58	0.900	−586.82	162.38	0.875	-560.38	146.73	0.91
120HCL	−504.12	94.00	0.895	−356.32	−182.75	0.951	-525.05	121.41	0.9
80LCL	−532.59	162.19	0.902	−562.74	124.16	0.919	-564.73	-86.0	1.0
100LCL	−534.31	172.33	0.908	−598.74	84.80	0.908	-732.85	3.590	.98
120LCL	−520.45	130.79	0.906	−600.49	87.80	0.942	-652.57	-66.51	0.98

The presence of pinholes in the membrane facilitates uncontrolled hydrogen crossover from the anode to the cathode, effectively mimicking the behavior of a faulty electrode. This results in disrupted electrochemical reactions and leads to significantly impaired reaction kinetics, as evidenced by increased Tafel slope values. Such conditions accelerate membrane degradation through localized hot spots and excessive water generation, ultimately causing premature fuel cell failure.
However, among the configurations studied, the CCFF-6 mm flow field exhibited consistently lower and more stable Tafel slope values, even in the presence of membrane pinholes. This suggests superior reaction kinetics, more efficient reactant utilization, and enhanced membrane durability. These results underscore the advantage of optimized flow field design in mitigating the adverse effects of structural defects and prolonging the operational life of PEM fuel cells.

3.2 Comparison of polarisation curve for MEA with pin-hole present

Polarization curves were generated for selected flow field and catalyst loading combinations under optimized operating conditions, based on prior experimental findings and unpublished work by the author. The following six configurations were selected to represent a diverse set of flow field geometries, catalyst loadings, and reactant flow rates:

CCFF-6 mm with higher catalyst loading: operating at 100 ml/min hydrogen flow rate with 100% excess oxygen, identified as the optimal condition from the author's previous unpublished data.

CCFF-6 mm with lower catalyst loading: operating at 80 ml/min hydrogen flow rate with 100% excess oxygen, representing the best performing combination for this configuration.

CCFF-4 mm with higher catalyst loading: operating at 80 ml/min hydrogen flow rate with 150% excess oxygen, chosen based on maximum power output in earlier trials.

CCFF-4 mm with lower catalyst loading: operating at 80 ml/min hydrogen flow rate with 100% excess oxygen.

Twin-Inlet Twin-Outlet Flow Field (TITOFF) with higher catalyst loading: operating at 80 ml/min hydrogen flow rate with 50% excess oxygen, identified as the optimal condition for this configuration.

TITOFF with lower catalyst loading: operating at 80 ml/min hydrogen flow rate with 100% excess oxygen, based on best observed performance.

These combinations were selected to provide a comparative understanding of the influence of flow field geometry, catalyst loading, and oxygen availability on the fuel cell's polarization behavior, particularly in the presence of membrane defects such as pinholes.

In addition to the previously discussed configurations, experiments were also conducted for the following cases:

CCFF-2 mm with higher catalyst loading: operated at 120 ml/min hydrogen flow rate with 150% excess oxygen.

CCFF-2 mm with lower catalyst loading: operated under the same conditions,120 ml/min hydrogen flow rate and 150% excess oxygen.

Conventional Serpentine Flow Field (CSFF).

However, in the last three cases, the fuel cell failed to maintain steady operation beyond the open-circuit voltage (OCV) condition. The recorded voltage, current, and power outputs were highly unstable or negligible, preventing the generation of reliable polarization curves. These results indicate significant performance limitations, likely due to a combination of factors such as inadequate gas distribution, severe flooding, excessive hydrogen crossover through pinholes, and insufficient electrochemical activity, particularly under high flow rate and low catalyst loading conditions.

The polarization curves for cases exhibiting significant limiting current density have been plotted in Figure 8 for three different hydrogen flow rates. In the Fig. 8, the curves are labeled as follows:

A represents 80 ml/min hydrogen flow rate,

B represents 100 ml/min, and

C represents 120 ml/min.

These curves enable a comparative analysis of cell performance across varying flow rates under conditions where meaningful electrochemical behaviour was observed.

Out of the ten different flow field–catalyst loading combinations studied, the following configurations were excluded from Fig. 8 due to the fuel cell's inability to sustain even minimal external loads.

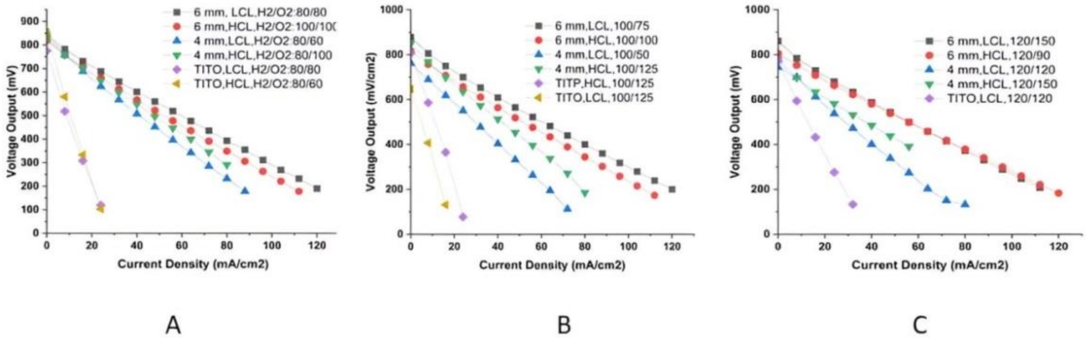

Fig. 8 Polarisation curve for PEMFC at best excess oxygen proportion with different flow field for catalyst loading at best hydrogen/oxygen proportion. A. 80 ml/min hydrogen flow rate, B. 100 ml/min flow rate, C. 120 ml/min(Different flow field used: 1) Circular cavity type flow field with 2 mm, 4 mm, and 6 mm cavity diameter; 2) Twin inlet –twin outlet(TITO) flow field 3) Conventional serpentine flow field. Different catalyst loading used: Higher catalyst loading (HCL)-0.25 mg/cm2 (anode) and 0.5 mg/cm2 (cathode), Lower catalyst loading (LCL)-0.2 mg/cm2 (anode) and 0.4 mg/cm2(cathode))

Conventional Serpentine Flow Field (CSFF) with both higher and lower catalyst loading, and CCFF-2 mm with both higher and lower catalyst loading.

In these cases, excessive water accumulation in the cathode severely hindered oxygen transport, while significant hydrogen crossover through pinholes limited the availability of hydrogen at the anode for electrochemical reaction.

Additionally, for Figure 8C, the Twin-Inlet Twin-Outlet Flow Field (TITOFF) with higher catalyst loading was excluded, as the fuel cell failed to maintain stable operation or carry load under this configuration.

In Figure 8, the polarization curves corresponding to the CCFF-6 mm flow field for both higher and lower catalyst loading are observed to lie closely together across all hydrogen flow rates, indicating consistent performance and relatively stable electrochemical characteristics. Notably, at the 80 ml/min flow rate, the curve for the CCFF-4 mm configuration also lies close to those of the CCFF-6 mm, suggesting minimal variation in performance under low flow rate conditions.

However, at higher hydrogen flow rates (100 and 120 ml/min), increased hydrogen crossover through the pinholes appears to impede electron transport, thereby increasing ohmic losses. Although Tables 1 and 2 report ohmic loss values, these do not always align with the observed polarization trends, particularly for the 4-mm flow field, likely due to differences in limiting current density, which affects total load-bearing capability.

The Twin-Inlet Twin-Outlet Flow Field (TITOFF), a variant of the conventional serpentine design, exhibits a non-standard polarization curve, lacking a clear limiting current region. This irregularity can be attributed to severe flooding on both the anode and cathode sides. The flooding is primarily caused by parasitic hydrogen-oxygen reactions resulting from gas crossover, leading to excess water generation and instability in gas delivery to the membrane electrode assembly (MEA). This inconsistent water content likely disrupts local reaction rates and causes voltage fluctuations during operation.

Further, from the data in Tables 1 and 2 and Figure 8, it is evident that open-circuit voltages (OCVs) for all CCFF configurations are consistently higher than those observed for the TITOFF configuration. For example:

- CCFF OCVs range from 890 to 1013 mV,
- While TITOFF OCVs range from 647 to 807 mV.

This difference indicates a greater degree of hydrogen crossover in TITOFF, leading to more rapid performance degradation. Moreover, as the experiments were conducted without external heating, the low operating temperatures of the PEMFC further contributed to voltage losses, especially at open circuit. Although the absolute hydrogen flow rates were low, the difference in crossover effects between CCFF and TITOFF designs significantly impacted OCVs. This underscores the high sensitivity of OCV to hydrogen crossover, particularly in low-temperature PEM fuel cells.

3.3 Effect of pin-hole on key performance parameters

The reduction in key performance parameters including open-circuit voltage (OCV), activation overpotential, ohmic overpotential, and maximum power output as a result of using membranes with pinhole defects is summarized in Table 4. These reductions underscore the detrimental impact of pinholes on overall fuel cell performance and durability.

Table 4

Difference in performance for the PEMFC with normal and pin-hole operation (Variables considered are open circuit voltage, activation and ohmic overpotential, and maximum power,NWD:Not well defined;NSV:no steady value)

		CCFF-6 mm		CCFF-4mm		CCFF-2 mm		TTFF		CS	
		LCL	HCL	LCL	HCL	LCL	HCL	LCL	HCL	LCL	HCL
OCV	80	970	890	1002	976	980	922	958	976	951	926
	100	940	921	983	976	965	933	971	1038	958	922
	120	915	890	1013	940	952	987	970	897	976	888
OCV (With pin hole)	80	860	812	846	861	822	796	775	855	NWD	NWD
	100	878	818	762	850	842	848	647	807	NWD	NWD
	120	861	806	724	780	804	848	771	-	NWD	NWD
Reduction in OCV for MEA with pin hole(%)	80	11.3	8.7	15.5	11.7	16.1	13.6	19.1	12.3	NWD	NWD
	100	6.5	11.1	22.4	12.9	12.7	9.1	33.3	22.2	NWD	NWD
	120	5.9	9.4	28.5	17.0	15.5	14.0	20.5	-	NWD	NWD
Activation Over Potential	80	299	417	311	317	320	342	433	271	401	388
	100	190	347	409	181	416	437	434	600	452	373
	120	316	236	299	299	379	481	448	445	485	320
Activation over potential with Pin-hole	80	300	268	339	71	-	128	NWD	NWD	NWD	NWD
	100	269	254	0	82	363	146	NWD	NWD	NWD	NWD
	120	273	184	0	146	-	134	NWD	NWD	NWD	NWD
Reduction in AAOP for	80	-0.33	35.7	-9.0	77.6	-	62.5	-	NWD	NWD	NWD

MEA with pin hole(%)	100	-41.5	26.8	100	54.6	12.7	66.5	-	NWD	NWD	NWD
	120	13.6	22.0	100	51.1	-	72.1	-	NWD	NWD	NWD
Ohmic Over potential	80	562	297	543	368	529	457	357	162	374	381
	100	620	377	378	495	415	367	347	180	213	351
	120	423	445	530	384	465	381	345	308	308	388
Ohmic Over potential with pin hole	80	370	383	329	381	-	494	-	NWD	NWD	NWD
	100	365	346	650	638	224	549	-	NWD	NWD	NWD
	120	337	439	606	243	-	528	-	NWD	NWD	NWD
Reduction in OVP(%)	80	34.1	-28.9	39.4	-3.5	-	-8.0	-	NWD	NWD	NWD
	100	41.1	8.2	-71.9	-28.8	46.0	-49.5	-	NWD	NWD	NWD
	120	20.3	1.3	-14.3	36.7	-	-38.5	-	NWD	NWD	NWD
Maximum power (mW)	80	781	774	670	743	590	274	564	590	568	590
	100	800	847	809	843	512	521	704	833	560	635
	120	771	818	795	770	560	324	565	493	538	705
Maximum Power with pin-hole(mW)	80	737	643	555	638	-	545	122	132	NWD	NWD
	100	687	700	402	553	156	632	81	146	NWD	NWD
	120	748	759	406	547	174	714	172	NSV	NWD	NWD
Reduction in Max.power with pin hole(%)	80	5.6	16.9	17.1	14.1	-	-98.9	78.3	77.6	-	-
	100	14.1	17.3	50.3	34.4	69.5	-21.3	88.4	82.4	-	-
	120	2.9	7.2	48.9	28.9	68.9	-120.3	69.5	-	-	-

Table 4 presents a comparative summary of key performance variables for fuel cells operating with a regular membrane electrode assembly (MEA) and with an MEA containing a pinhole defect. While some data points in Table 4 appear as outliers, not following the general trend, they are retained for completeness and reflect the variability introduced by membrane damage.

The general observation is that, for most flow field configurations, the introduction of a pinhole leads to unstable or inconsistent values across key parameters. However, configurations such as CCFF-6 mm, and to a lesser extent CCFF-4 mm, demonstrate relatively steady performance even with pinhole presence, suggesting better tolerance to membrane degradation.

Across the board, the results indicate a notable reduction in: Open-circuit voltage (OCV), Activation overpotential, Ohmic losses, and Maximum power output, when operating with a pinhole-damaged membrane. These reductions highlight the detrimental impact of membrane defects on fuel cell efficiency and reinforce the importance of robust flow field design in mitigating performance loss due to mechanical degradation.

4. CONCLUSION

The following conclusions have been drawn based on the study:

Certain flow field configurations continue to deliver reasonably good performance even with the presence of membrane pin-holes. This suggests that such configurations offer improved durability for the fuel cell system.

The presence of pin-holes in the membrane results in reduced open circuit voltage (OCV) and maximum power output. Specifically, the OCV decreased by 41.1%, while the maximum power declined by 69.5% compared to a membrane without defects. Furthermore, flow field configurations such as CCFF-2 mm, TITOFF, and CS exhibited unsteady performance when used with pin-holed membranes.

Among the tested configurations, the CCFF-6 mm flow field demonstrated the best performance under pin-hole conditions. It delivered higher OCV, improved voltage and power at load, superior maximum power output, greater limiting current density, and a better-defined maximum power point than all other configurations.

The presence of pin-holes facilitates hydrogen crossover, which in turn leads to increased cell temperature and enhanced water production, adversely affecting performance and durability.

A hydrogen flow rate of 80 mL/min resulted in the least flooding and lower heat generation, making it the most effective among the tested flow rates under the given conditions.

Across all tested hydrogen flow rates, the CCFF-2 mm configuration was unable to sustain significant external loads, rendering it practically inoperative. This severe performance loss is attributed to i)The small diameter of the circular cavities hindered effective reactant delivery to the membrane electrode assembly (MEA), leading to inadequate gas distribution, ii) Pin-holes enabled direct hydrogen crossover to the cathode side, causing parasitic chemical reactions and excess water generation, iii) Low catalyst loading further reduced the number of active reaction sites, compounding the overall inefficiency.

The Tafel slope analysis suggests that the CCFF-6 mm configuration exhibits superior reaction kinetics compared to CCFF-4 mm and CCFF-2 mm configurations, further supporting its efficacy in maintaining performance under adverse conditions. The combined effect of low temperature and hydrogen crossover has adverse effect on the reaction kinetics and hence output variables are lower than that of normal operation.

ACKNOWLEDGEMENTS

The author places on record his gratefulness to All India Council for Technical Education for providing financial support to carry out the research.

REFERENCES

Bodner, M., Hochenauer, C., & Hacker, V., 2015. Effect of pinhole location on degradation in polymer electrolyte fuel cells. Journal of Power Sources, 295, 336–348.

Büchi, F. N., & Srinivasan, S., 1997. Operating proton exchange membrane fuel cells without external humidification of the reactant gases: Fundamental aspects. Journal of the Electrochemical Society, 144(8), 2767–2772. DOI: 10.1149/1.1837893

Chen, J., Luo, Y., Zhang, L., Kwan, T. H., & Yao, Q., 2025. Multi-physics pinhole size tolerance analysis on the leakage characteristics and performance of proton exchange membrane fuel cells. Energy Science & Engineering, 3, 4402–4416. DOI: 10.1002/ese3.70183

Chippar, P., Oh, K., Kim, W.-G., & Ju, H., 2014. Numerical analysis of effects of gas crossover through membrane pinholes in high-temperature proton exchange membrane fuel cells. International Journal of Hydrogen Energy, 39(6), 2863–2871.

Collier, A., Wang, H., Yuan, X. Z., Zhang, J., & Wilkinson, D. P., 2006. Degradation of polymer electrolyte membranes. International Journal of Hydrogen Energy, 31(13), 1838–1854. DOI: 10.1016/j.ijhydene.2006.05.006

De Moor, G., Bas, C., Charvin, N., Moukheiber, E., Niepceron, F., Breilly, N., André, J., Rossinot, E., Claude, E., Albérola, N. D., & Flandin, L., 2012. Understanding membrane failure in PEMFC: Comparison of diagnostic tools at different observation scales. Fuel Cells, 12(3), 356–364. DOI: 10.1002/fuce.201100161

Ding, F., Zou, T., Wei, T., Chen, L., Qin, X., Shao, Z., & Yang, J., 2023. The pinhole effect on proton exchange membrane fuel cell (PEMFC) current density distribution and temperature distribution. Applied Energy, 342, Article 121136.

Ehlinger, V. M., Kusoglu, A., & Weber, A. Z., 2019. Modeling coupled durability and performance in polymer-electrolyte fuel cells: Membrane effects. Journal of The Electrochemical Society.

Endoh, E., Terazono, S., Widjaja, H., & Takimoto, Y., 2004. Degradation study of MEA for PEMFCs under low humidity conditions. Electrochemical and Solid-State Letters, 7, A209–A211.

Kusoglu, A., Karlsson, A. M., Santare, M. H., Cleghorn, S., & Johnson, W. B., 2006. Mechanical response of fuel cell membranes subjected to a hygro-thermal cycle. Journal of Power Sources, 161(2), 987–996. DOI: 10.1016/j.powsour.2006.05.020

Lai, Y., Mittelsteadt, C. K., Gittleman, C. S., & Dillard, D. A., 2009. Viscoelastic stress analysis of constrained proton exchange membranes under humidity cycling. Journal of Fuel Cell Science and Technology, 6(2), Article 021002. DOI: 10.1115/1.2971045

Meredith, M. T., Kao, D.-Y., Hickey, D., Schmidtke, D. W., & Glatzhofer, D. T., 2011. High current density ferrocene-modified linear poly(ethylenimine) bioanodes and their use in biofuel cells. Journal of the Electrochemical Society, 158(2), B166–B174. DOI: 10.1149/1.3505950

Moukheiber, E., Bas, C., & Flandin, L., 2014. Understanding the formation of pinholes in PFSA membranes with the essential work of fracture (EWF). International Journal of Hydrogen Energy, 39(6), 2717–2723. DOI: 10.1016/j.ijhydene.2013.03.031

Nguyen, T.-T., & Fushinobu, K., 2020. Effect of operating conditions and geometric structure on gas crossover in PEM fuel cells. Sustainable Energy Technologies and Assessments, 37, Article 100584.

Silberstein, M. N., & Boyce, M. C., 2011. Hygro-thermal mechanical behavior of Nafion during constrained swelling. Journal of Power Sources, 196(7), 3452–3460. DOI: 10.1016/j.jpowsour.2010.11.116

Tang, Y., Karlsson, A. M., & Santare, M. H., 2006. An experimental investigation of humidity and temperature effects on the mechanical properties of perfluorosulfonic acid membrane. Materials Science and Engineering A, 425(1–2), 297–304.

Yu, J., 2005. In situ analysis of performance degradation of a PEMFC under nonsaturated humidification. Electrochemical and Solid-State Letters, 8, A156.

Yu, J., Matsuura, T., Yoshikawa, Y., Islam, M. N., & Hori, M., 2005. Lifetime behavior of a PEM fuel cell with low humidification of feed stream. Physical Chemistry Chemical Physics, 7(2), 373–378.

Zhang, S., Yuan, X.-Z., Hin, J., Wang, H., Friedrich, K. A., & Schulze, M., 2009. A review of platinum-based catalyst layer degradation in proton exchange membrane fuel cells. Journal of Power Sources, 194(2), 588–600. DOI: 10.1016/j.jpowsour.2009.06.073